



SUBGRID SNOW DEPTH COEFFICIENT OF VARIATION SPANNING ALPINE TO SUB-ALPINE MOUNTAINOUS TERRAIN

GRAHAM A. SEXSTONE^{1,2} , STEVEN R. FASSNACHT^{1,2,3*} ,
JUÁN I. LÓPEZ-MORENO⁴ , CHRISTOPHER A. HIEMSTRA⁵ 

¹ ESS-Watershed Science, Colorado State University, USA.

² Natural Resources Ecology Laboratory, Colorado State University, USA.

³ Cooperative Institute for Research in the Atmosphere, USA.

⁴ Instituto Pirenaico de Ecología, Spain.

⁵ U.S. Army Cold Regions Research and Engineering Laboratory, USA.

ABSTRACT. Given the substantial variability of snow in complex mountainous terrain, a considerable challenge of coarse scale modeling applications is accurately representing the subgrid variability of snowpack properties. The snow depth coefficient of variation (CV_{ds}) is a useful metric for characterizing subgrid snow distributions but has not been well defined by a parameterization for mountainous environments. This study utilizes lidar-derived snow depth datasets spanning alpine to sub-alpine mountainous terrain in Colorado, USA to evaluate the variability of subgrid snow distributions within a grid size comparable to a 1000 m resolution common for hydrologic and land surface models. The subgrid CV_{ds} exhibited a wide range of variability across the 321 km² study area (0.15 to 2.74) and was significantly greater in alpine areas compared to subalpine areas. Mean snow depth was the dominant driver of CV_{ds} variability in both alpine and subalpine areas, as CV_{ds} decreased nonlinearly with increasing snow depths. This negative correlation is attributed to the static size of roughness elements (topography and canopy) that strongly influence seasonal snow variability. Subgrid CV_{ds} was also strongly related to topography and forest variables; important drivers of CV_{ds} included the subgrid variability of terrain exposure to wind in alpine areas and the mean and variability of forest metrics in subalpine areas. Two statistical models were developed (alpine and subalpine) for predicting subgrid CV_{ds} that show reasonable performance statistics. The methodology presented here can be used for characterizing the variability of CV_{ds} in snow-dominated mountainous regions, and highlights the utility of using lidar-derived snow datasets for improving model representations of snow processes.

Coficiente de variación del espesor de la nieve a escala de subcuadrícula en áreas montañosas alpinas y subalpinas

RESUMEN. Dada la variabilidad de la nieve en áreas de montaña complejas, un reto importante de las aplicaciones de modelado a gran escala es representar con precisión la variabilidad de las propiedades de la capa de nieve a escala de subcuadrícula. El coeficiente de variación (CV_{ds}) del espesor de la nieve es una medida útil para caracterizar la distribución de la nieve en subcuadrículas, pero no ha sido bien definido mediante una parametrización para entornos montañosos. Este estudio utiliza datos de espesor de la nieve derivados de LIDAR en áreas montañosas alpinas y subalpinas de Colorado, EE. UU. La finalidad es evaluar la variabilidad de la distribución de la nieve a escala de subcuadrícula dentro de un tamaño de cuadrícula de una resolución de 1000 m habitual para modelos hidrológicos y de superficie del terreno. Los CV_{ds} de la subcuadrícula mostraron un amplio rango de variabilidad en el área de estudio de 321 km² (0,15 a 2,74) y fueron significativamente mayores en las

áreas alpinas en comparación con las áreas subalpinas. El espesor medio de la nieve fue el factor determinante de la variabilidad del CV_{ds} tanto en áreas alpinas como subalpinas, ya que el CV_{ds} disminuyó de forma no lineal con el incremento del espesor de la nieve. Esta correlación negativa se atribuye al tamaño estático de los elementos rugosos (topografía y dosel) que influyen fuertemente en la variabilidad estacional de la nieve. El CV_{ds} de la subcuadrícula también estuvo muy relacionado con la topografía y las variables forestales. Los controladores determinantes del CV_{ds} fueron la variabilidad a escala de subcuadrícula de la exposición del terreno al viento en áreas alpinas y la media y variabilidad de las métricas forestales en áreas subalpinas. Se desarrollaron dos modelos estadísticos (alpino y subalpino) para predecir el CV_{ds} a escala de subcuadrícula que muestran estadísticamente rendimientos razonables. La metodología presentada aquí puede ser utilizada para caracterizar la variabilidad de CV_{ds} en regiones montañosas dominadas por la nieve, y subraya la utilidad de usar conjuntos de datos de nieve derivados de LIDAR para mejorar las representaciones de modelos de procesos de nieve.

Key words: Snow distribution, subgrid variability, coefficient of variation, lidar, modeling.

Palabras clave: Distribución de la nieve, variabilidad de la subcuadrícula, coeficiente de variación, lidar, modelos.

Received: 9 December 2020

Accepted: 19 April 2021

Corresponding author: Steven R. Fassnacht. ESS-Watershed Science, Colorado State University. E-mail address: steven.fassnacht@colostate.edu

1. Introduction

Snow plays an important role in hydrological, ecological, and atmospheric processes within much of the Earth System, and for this reason, considerable research has focused on understanding the spatial and temporal distribution of snow depth (d_s) and snow water equivalent (SWE) across the landscape (Clark *et al.*, 2011). Snowpacks tend to exhibit substantial spatiotemporal variability (López-Moreno *et al.*, 2015) that is shaped by processes at varying spatial scales (Blöschl, 1999). The variability of the snowpack through space and time at a given scale of interest is often driven by meteorology and its interactions with topography and forest features as well as land-cover changes from forest disturbance and deforestation (Berris and Harr, 1987). Mountainous areas, which often accumulate large seasonal snowpacks, generally exhibit a high range of snow variability because of these effects (Sturm *et al.*, 1995). Given that this variability occurs over relatively short distances (Fassnacht and Deems, 2006; López-Moreno *et al.*, 2011), accurately modeling the distribution of snow in mountainous areas requires a detailed understanding of the characteristics of snow variability at the model scale of interest (Trujillo and Lehning, 2015).

An important challenge of physically-based modeling is often the ability to represent subgrid processes, or the spatial variability of critical input parameters (Seyfried and Wilcox, 1995). Accurate representation of subgrid snow distribution is critical for reliably simulating energy and mass exchanges between the land and atmosphere in snow-covered regions (Liston, 1999), yet various studies have highlighted a deficiency with this representation in hydrologic and land-surface models (Pomeroy *et al.*, 1998; Slater *et al.*, 2001; Liston, 2004; Clark *et al.*, 2011; Liston and Hiemstra, 2011). Liston (2004) presented an approach of effectively representing subgrid snow distributions in coarse-scale models by using a lognormal probability density function and an assigned coefficient of variation (CV). This approach only requires an estimation of the CV parameter (i.e. standard deviation divided by the mean), which has generally been estimated from field data and is a measure of snow variability that allows for comparisons that are independent of the amount of snow accumulation. Representative values of the CV

of snow water equivalent (CV_{SWE}) and snow depth (CV_{ds}) have been published by many field studies (refer to Table 1 and Figure 2 from Clark *et al.*, 2011) and have been summarized based on vegetation and landform type (Pomeroy *et al.*, 1998) and classified globally, based on air temperature, topography, and wind speed regimes (Liston, 2004). However, the range of published CV_{SWE} and CV_{ds} in complex mountainous terrain (i.e. the mountain snow class from Sturm *et al.*, 1995) is quite variable and a parameterization has not been well defined.

The recent developments of snow depth mapping capabilities from ground-based and airborne lidar (Deems *et al.*, 2013) as well as digital photogrammetry (Bühler *et al.*, 2015; Nolan *et al.*, 2015) have provided a high definition view of snow depth distributions, albeit at fixed locations in space and time, that have not been historically available by traditional field measurements. These detailed snow depth datasets have aided in an improved understanding of the scaling properties of snow distributions (Deems *et al.*, 2006; Trujillo *et al.*, 2007), the temporal evolution of snow distributions (Grünwald *et al.*, 2010; López-Moreno *et al.*, 2015), the relation of snow depth with topography (Grünwald *et al.*, 2013; Kirchner *et al.*, 2014; Revuelto *et al.*, 2014) and canopy (Broxton *et al.*, 2015; Revuelto *et al.*, 2015; Zheng *et al.*, 2016) characteristics, as well as the nature of fine scale subgrid variability of snow depth (López-Moreno *et al.*, 2015). Grünwald *et al.* (2013) present a novel study in which lidar-derived snow depth datasets are aggregated to coarse scale grids to evaluate the drivers of snow distribution at the catchment scale. Evaluations of lidar snow depth datasets within coarser scale grid resolutions can be analogous to the grid resolution of many modeling applications, thus lidar-derived snow datasets have potential to serve as an important tool for evaluating the representation of subgrid snow distributions within physically-based models.

In this study, we evaluate the snow depth coefficient of variation (CV_{ds}) as a metric of subgrid snow variability within complex mountainous terrain spanning alpine to sub-alpine land covers in north-central Colorado, U.S.A. We evaluate CV_{ds} at a grid resolution comparable to 1000 m resolution of hydrologic and land surface models. The objectives of this research were to (1) determine the range of CV_{ds} values that are observed within varying grid resolutions throughout the study area, (2) evaluate the effects of mean snow depth, forest, and terrain characteristics on subgrid CV_{ds} , and (3) develop a methodology for characterizing CV_{ds} within complex mountainous terrain. This research aims to help advance understanding of the variability of subgrid snow distributions, and inform more accurate representations of subgrid snow variability that can be used within physically-based models.

2. Methods

2.1. Site description

This research was conducted in the Front Range Mountains of north-central Colorado, located in the western United States (Fig. 1). Spatial lidar datasets collected by the Boulder Creek Critical Zone Observatory (CZO) (<http://criticalzone.org/boulder/>, accessed 17 April 2016) were investigated in this study. The study area ranges in elevation from 2190 m to 4117 m and is dominated by ponderosa pine (*Pinus ponderosa*) and lodgepole pine (*Pinus contorta*) forests at lower elevations; Engelmann spruce (*Picea engelmannii*) and subalpine fir (*Abies lasiocarpa*) forests at higher elevations, and alpine tundra at the highest elevations (Fig. 1). The mean winter (1 October to 1 May) precipitation and temperature for water years 2006-2010 at the Niwot SNOTEL site (3021 m; Fig. 1) is 452 mm and 2.7°C (Harpold *et al.*, 2014). The mountainous terrain in this region is complex, varying from gentle topography at lower elevations to steep and rugged slopes closer to the Continental Divide. The majority of the study area has a southeastern aspect and is located on the eastern side of the Continental Divide (Fig. 1). The Front Range Mountains are characterized by a continental seasonal snowpack (Trujillo and Molotch, 2014), with the persistent snow zone at elevations greater than 3050 m (Richer *et al.*, 2013), generally exhibiting peak snow accumulation during the springtime months of April and May each year.

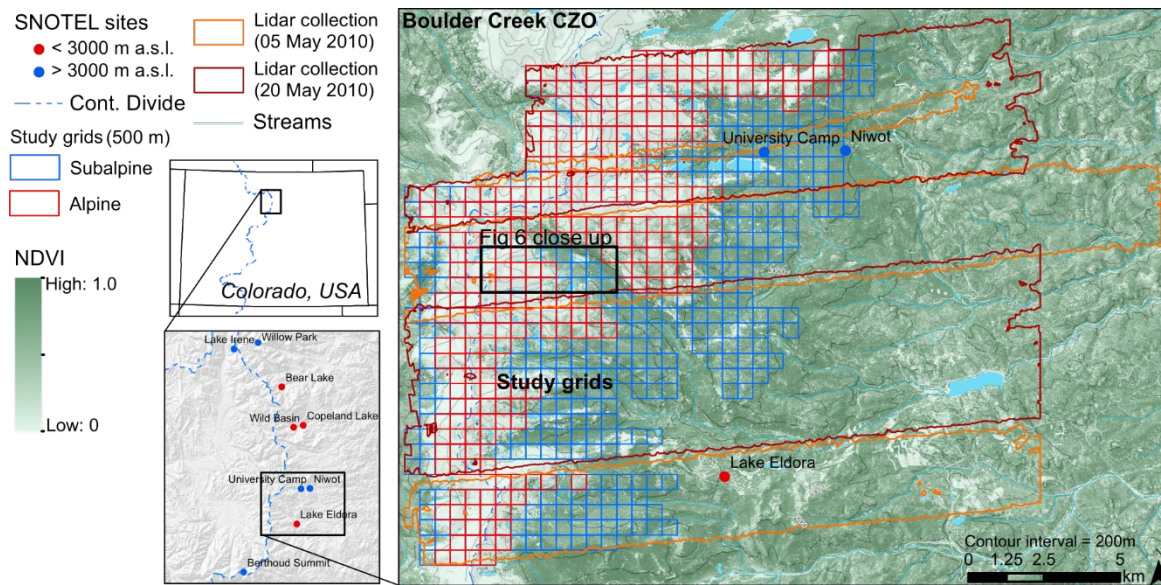


Figure 1. Map of the Boulder Creek CZO study area located within the Front Range Mountains of northern Colorado, USA. NRCS SNOTEL sites in the region are shown in blue (sites greater than 3000 m elevation) and red (sites less than 3000 m elevation). The extent of the snow-covered lidar collection on 05 May 2010 (20 May 2010) is shown in orange (red). The 500 m resolution study grids ($n = 642$) are shown in gray. The blue rectangle highlights the area of close up shown in Figure 5.

2.2. Spatial datasets

This study uses the publicly available lidar-derived snow depth (d_s), elevation (z), and vegetation height (VH) raster datasets (1 m resolution) from the Boulder Creek CZO (ftp://snowserver.colorado.edu/pub/WesternCZO_LiDAR_data, accessed 27 August 2015) that are described in detail by Harpold *et al.* (2014). Airborne lidar campaigns were completed during snow-covered (May 2010) and snow free (August 2010) periods across the study area and lidar surfaces were differenced to derive d_s (Harpold *et al.*, 2014). The snow-covered lidar returns were collected on two dates, 05 May 2010 and 20 May 2010, and the combined snow-covered lidar extent is 321 km² (Fig. 1). A comparison of the lidar d_s dataset to in situ d_s sensors within research catchments in the Boulder Creek CZO showed a Root Mean Squared Error (RMSE) of 27 cm (44% relative to lidar catchment mean) and 7 cm (117% relative to lidar catchment mean) at the Como Creek catchment (16 sensors) and Gordon Gulch catchment (5 sensors), respectively (Harpold *et al.*, 2014).

The lidar-derived digital elevation model (DEM) was resampled from a 1 m to a 10 m resolution for representation of the resolution of commonly available DEMs (USGS National Elevation Dataset, <http://ned.usgs.gov>) and was subsequently used to derive terrain variables for each 10 m cell that have been shown to influence d_s distributions (Elder *et al.*, 1998; Winstral *et al.*, 2002; Erickson *et al.*, 2005; Kerr *et al.*, 2013; Revuelto *et al.*, 2014) using a Geographic Information System (GIS). Surface slope (S) was calculated by fitting a plane to a 3 x 3 cell window around each DEM cell. Winter clear-sky incoming solar radiation ($Q_{sw\downarrow}$) was determined using the Area Solar Radiation tool in ArcGIS, which calculates mean incoming solar radiation for clear-sky conditions across a DEM surface for a specified time interval based on solar zenith angle and terrain shading. The time interval used for the calculation of $Q_{sw\downarrow}$ was 01 October through 01 May. Aspect was not considered because it was highly correlated with $Q_{sw\downarrow}$. Maximum upwind slope (S_x) (Winstral *et al.*, 2002), which can be used as a measure of the exposure to or sheltering from wind, was calculated for each cell as:

$$S_{x,d\max}(x_i, y_i) = \max \left(\tan^{-1} \left\{ \frac{z(x_v, y_v) - z(x_i, y_i)}{\left[(x_v - x_i)^2 + (y_v - y_i)^2 \right]^{0.5}} \right\} \right) \quad (1)$$

where α is the azimuth of the search direction, d_{max} is the maximum distance for the search direction, z is elevation, and (x_v, y_v) are all cells along the vector defined by α and d_{max} . Given the prevailing westerly winds within the study area (Winstral *et al.*, 2002; Erickson *et al.*, 2005], an average S_x was calculated for a d_{max} of 200 m and a range of α from 240° to 300° at 5° increments (Molotch *et al.*, 2005). Topographic position index (*TPI*) (Weiss, 2001), which is a measure of the relative position of the cell to surrounding terrain, was calculated for each cell as:

$$TPI = z_0 - \bar{z} \quad (2)$$

$$\bar{z} = \frac{1}{n_R} \sum_{i \in R} z_i \quad (3)$$

where z_0 is the elevation of the cell and \bar{z} is the average elevation of the surrounding cells within a specified cell window (R). *TPI* was calculated for 3 x 3 (i.e. 30 m resolution), 11 x 11, and 21 x 21 windows around each cell. Additionally, a 30 m resolution 2011 canopy density (*CD*) dataset was downloaded for the study area (<http://www.mrlc.gov/nlcd2011.php>, accessed 04 December 2015).

2.3. Aggregation of study grids

Operational snow models (Carroll *et al.*, 2006] often have a 1000 m horizontal grid resolution and snow representations within land surface models (Slater *et al.*, 2001) have generally been designed for a coarser resolution (Yang *et al.*, 1997) but are being developed to operate at finer scales (Kumar *et al.*, 2006; Wood *et al.*, 2011; Bierkens *et al.*, 2015). This study attempts to evaluate the subgrid variability of d_s at a comparable grid resolution to this 1000 m model grid size. Therefore, the subgrid variability of d_s within study grids of 100 m, 200 m, 300 m, 400 m, 500 m, 750 m, and 1000 m resolutions was evaluated. For example, subgrid statistics for each 500 m study grid (with 100% d_s coverage) were calculated based on 250000 lidar-derived d_s cells. The goal of this was to identify an appropriate grid size for evaluation that exhibited similar characteristics of snow variability to the 1000 m resolution grids, but maximized the number of grids available for analysis within the study area. At least 80% coverage of each study grid by the lidar d_s datasets was required, and the d_s dataset with the greatest coverage was utilized for cases of the overlapping snow-covered lidar datasets (Fig. 1). When the 05 May 2010 and 20 May 2010 lidar d_s datasets were overlapping and both datasets had 100% study grid coverage, the 05 May 2010 dataset was used.

For each study grid, the mean and standard deviation (σ) of d_s were determined and used to calculate CV_{d_s} . The mean and standard deviation of each of the terrain and canopy variables outlined above were also calculated for each study grid. A categorical variable representing ecosystem type was also determined for each study grid. The alpine ecosystem type was assigned to study grids that had a mean elevation greater than 3300 m and a mean *VH* less than 0.5 m, while the remaining study grids were assigned to the subalpine ecosystem type; treeline elevation in this area generally varies between 3400 m and 3700 m (Suding *et al.*, 2015). Lastly, only study grids with a mean elevation greater than 3000 m (i.e. the persistent snow zone) were evaluated in this study. Table 1 provides a list of all variables used in this study.

Table 1. Symbols of variables and metrics used in this study.

Symbol	Variable
CV_{d_s}	snow depth coefficient of variation
d_s	snow depth
σ_{d_s}	standard deviation of snow depth
<i>VH</i>	vegetation height

σ_{VH}	standard deviation of vegetation height
CD	canopy density
σ_{CD}	standard deviation of canopy density
z	elevation
σ_z	standard deviation of elevation
S	surface slope
σ_S	standard deviation of surface slope
$Q_{sw\downarrow}$	winter clear-sky incoming solar radiation
$\sigma_{Q_{sw\downarrow}}$	standard deviation of winter clear-sky incoming solar radiation
S_x	maximum upwind slope
σ_{S_x}	standard deviation of maximum upwind slope
TPI	topographic position index
σ_{TPI}	standard deviation of topographic position index

2.4. Statistical analysis

Pairwise relations between CV_{d_s} and d_s , terrain variables and vegetation variables were explored for both alpine and subalpine study grids to evaluate drivers of subgrid d_s variability. CV_{d_s} was expected to have a strong nonlinear relation with d_s (Fassnacht and Hultstrand, 2015); therefore, this relation was detrended for both the alpine and subalpine study grids, and residuals were used to evaluate further terrain and vegetation effects on CV_{d_s} using Pearson's r coefficient. Additionally, multiple linear regression models (refer to Table 3 for general model equation) were developed to predict CV_{d_s} for both alpine and subalpine study grids based on the variables presented in Table 1. Variables included in the models were selected by an all-subsets regression procedure in which both Mallows' C_p (Mallows, 1973) and Akaike information criterion (AIC) (Akaike, 1974) were used as a measure of relative goodness of fit of the models (Sexstone and Fassnacht, 2014). Final independent variables within the models were required to be statistically significant (p value < 0.05) and not exhibit multicollinearity. Multicollinearity was defined as model parameters exhibiting a variance inflation factor greater than 2. Given that a non-normal distribution of snow depth (Liston, 2004) and other terrain and vegetation variables was expected, natural log and square root transformations of model variables (Table 1) were explored. Model diagnostics of residuals were used to ensure the model assumptions of normality, linearity, and homoscedasticity. Model performance was evaluated using the Nash-Sutcliffe efficiency (NSE) and RMSE. Additionally, model verification was assessed using a 10-fold cross-verification procedure which runs 10 iterations of removing a randomly-selected 10 percent of the dataset, fitting the regression to the remainder of the data, and subsequently comparing modeled values to the independent observations that were removed.

3. Results

3.1. Snowpack conditions

In a hypothetical uniform snowmelt scenario (Egli and Jonas, 2009), the subgrid mean d_s is expected to decrease faster than the σ_{d_s} , thus the CV_{d_s} will increase without a corresponding increase in subgrid snow variability (Winstral and Marks, 2014). Therefore, in this study, an evaluation of the snowpack conditions was important for assessing if the subgrid CV_{d_s} may have been influenced by a melting snowpack. SWE data from nine Natural Resources Conservation Service (NRCS) SNOTEL stations located in the Front Range Mountains of northern Colorado (Fig. 1) were evaluated to assess snowpack conditions. A snowmelt event occurred across the study area on 10 April 2010 (Fig. 2a) that caused considerable snowmelt at stations below an elevation of 3000 m and a loss of 10% of peak SWE on average at stations above 3000 m. Following this snowmelt event, substantial snow accumulation continued at SNOTEL stations above 3000 m until 17 May 2010, when the onset of snowmelt began

(Fig. 2a). A plot of σ_{ds} versus mean d_s among the SNOTEL stations highlights the hysteretic dynamics of accumulation and melt across the region (Egli and Jonas, 2009), and confirms that the lidar data were collected prior to and at the beginning of snowmelt across the study area (Fig. 2b). Given that the lidar-derived snow depth was collected before substantial snowmelt had occurred within the persistent snow zone, we are confident that the subgrid CV_{ds} evaluated in this study is representative of snow variability at peak snow accumulation in this region.

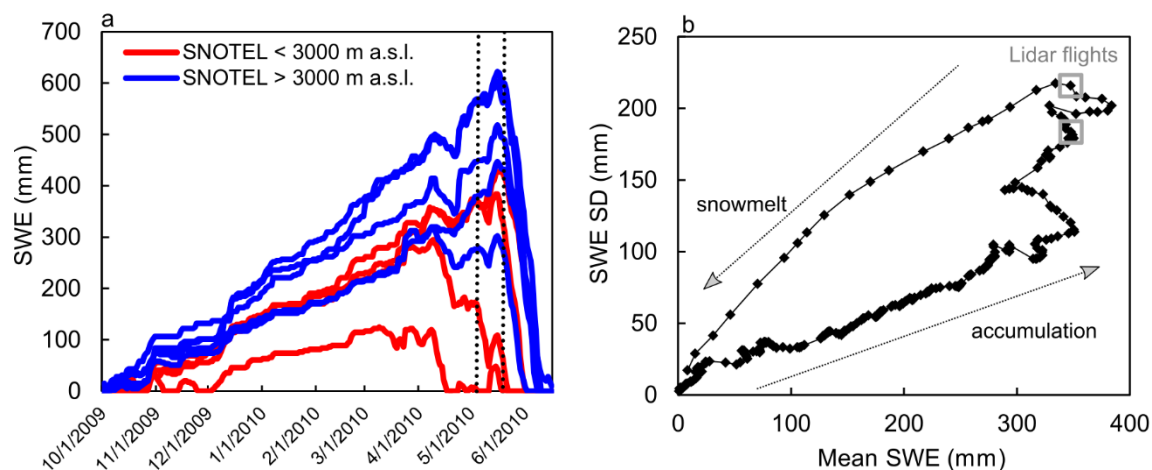


Figure 2. Snow water equivalent (SWE) data from nine NRCS SNOTEL sites within the region of the study area displayed as (a) niveographs showing snow accumulation and snowmelt throughout water year 2010 with the timing of 05 May 2010 and 20 May 2010 lidar flights plotted as vertical dashed lines and (b) a scatter plot of the standard deviation of SWE versus mean SWE from the SNOTEL sites highlighting the hysteretic dynamics of snow accumulation and snowmelt across the region based on nine SNOTEL stations (Egli and Jonas, 2009).

3.2. Subgrid snow depth variability

Snow depth CV (CV_{ds}) and σ_{ds} were consistently greater in the alpine versus subalpine at each of the varying grid resolutions (Fig. 3). The mean CV_{ds} across the study grids was generally consistent with changes in grid resolution; however, the standard deviation of CV_{ds} decreased with increasing grid resolution and stabilized around a 500 m grid size. The mean σ_{ds} across the study grids tended to increase with increasing grid size for all study grids, but stabilized around 400 m for subalpine study grids only. The 500 m resolution study grids ($n = 642$) were chosen for analysis in this study (Fig. 1) and is believed to be representative of the subgrid snow variability at the 1000 m resolution.

The median d_s , σ_{ds} , and CV_{ds} across all study grids (500 m resolution) was equal to 1.27 m, 0.88 m, and 0.74, respectively, and subgrid CV_{ds} ranged from 0.15 to 2.74 across the study area. The variability of CV_{ds} collected on 05 May 2010 ($n = 219$ study grids) and 20 May 2010 ($n = 423$ study grids) (Fig. 1) was similar, with the 05 May grids exhibiting a slightly smaller CV_{ds} (median = 0.64) than the 20 May grids (median = 0.81). Statistically significant differences (p value < 0.001) between the alpine and subalpine study grids were observed for d_s , σ_{ds} , and CV_{ds} by the nonparametric Mann-Whitney test (Fig. 4). The alpine study grids exhibited a greater mean and range of snow accumulation and variability than the subalpine study grids. The range of CV_{ds} from the 10th to the 90th percentiles within the alpine and subalpine study grids was equal to 0.61 to 1.57 and 0.30 to 0.98, respectively. Figure 5 highlights the abrupt change of subgrid snow depth variability characteristics observed in a transition from the subalpine to alpine ecosystem; the forest structure and terrain characteristics appears to exert a strong influence on subgrid CV_{ds} and these relations were investigated further.

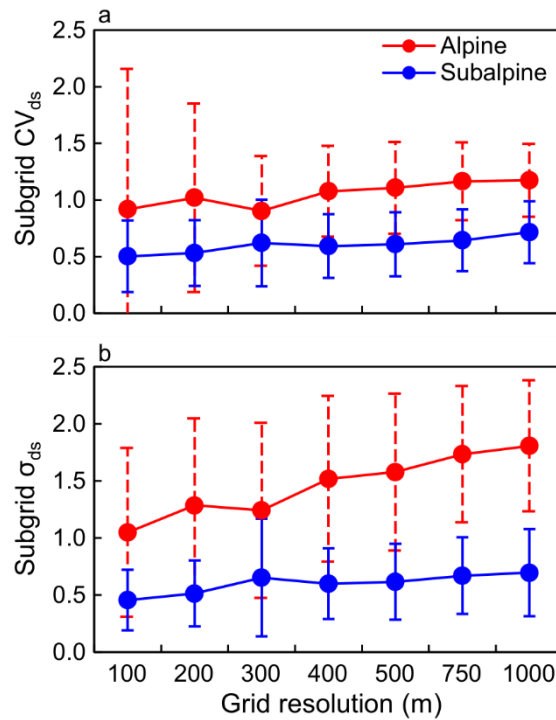


Figure 3. Mean subgrid (a) CV_{ds} and (b) σ_{ds} across the study area plotted versus study grid resolution for alpine (red) and subalpine (blue) study grids. Error bars represent the standard deviation of CV_{ds} and σ_{ds} across the study area.

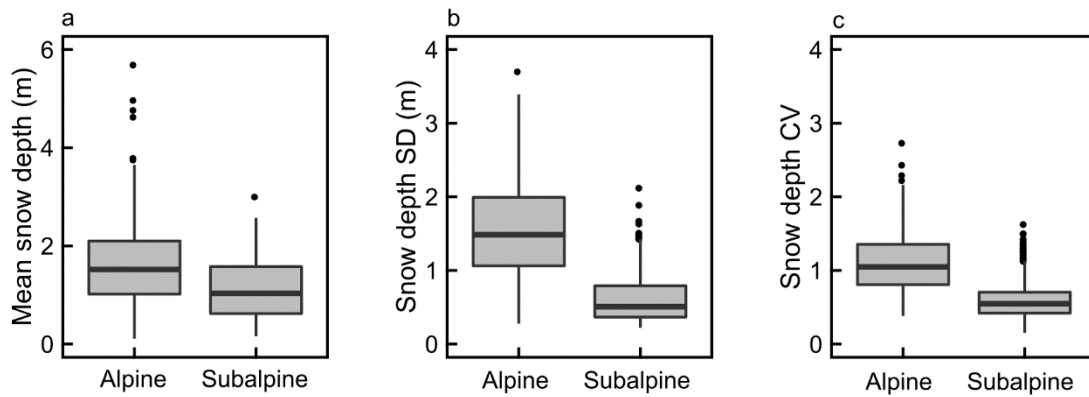


Figure 4. Boxplots showing the outliers (black circles), 10th and 90th percentiles (whiskers), 25th and 75th percentiles (box) and median (black horizontal line) for the (a) d_s , (b) σ_{ds} , and (c) CV_{ds} of the alpine and subalpine study grids (500 m resolution).

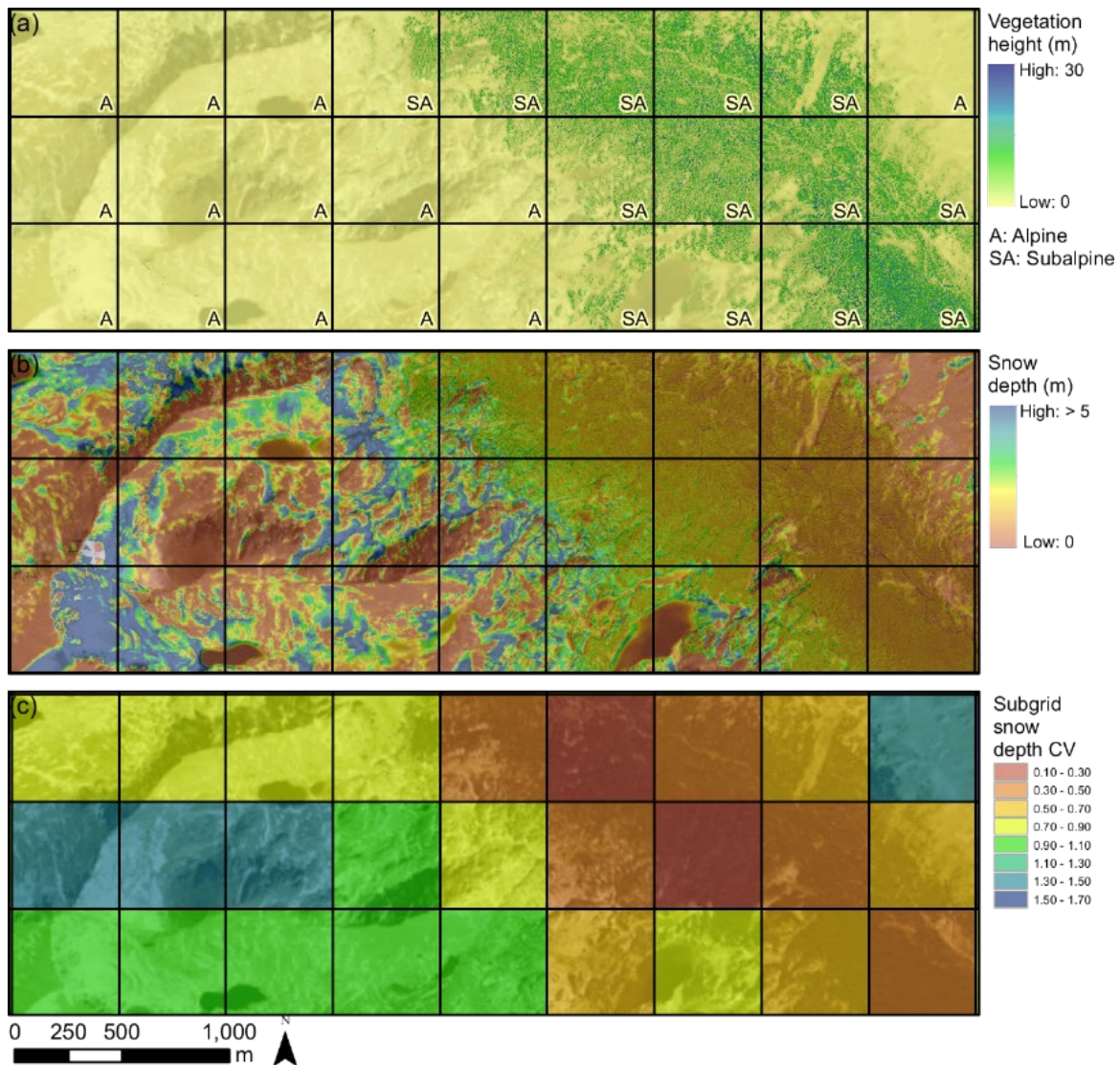


Figure 5. Close up map of selected study grids showing the distribution of (a) vegetation height and ecosystem type, (b) snow depth, and (c) subgrid CV_{ds} value. Area of close up is highlighted in Figure 1.

3.3. Relation of subgrid snow depth variability with terrain and forest characteristics

A statistically significant linear correlation (Pearson's r coefficient; p value < 0.05) between CV_{ds} and d_s was observed to be -0.60 and -0.45 for the alpine and subalpine study grids, respectively (Table 2). However, further evaluation showed this relation to be nonlinear and best described by a power function (Fig. 6). This function suggests that CV_{ds} exhibits a systematic decrease with increasing d_s and suggests that relative subgrid snow variability is importantly related to the total snow accumulation of a given year. The power relation between CV_{ds} and d_s was greatly improved when split between alpine and subalpine study grids, as a CV_{ds} for a corresponding d_s tended to be greater for alpine versus subalpine study grids (Fig. 6). The power functions (CV_{ds} versus d_s) were detrended (i.e. removing the influence of d_s on CV_{ds}) and the residuals of the functions were compared to terrain and forest characteristics (Table 2). The alpine study grids were most positively correlated with σ_{sx} suggesting that the variability of wind exposure and sheltering and thus wind redistribution within a study grid is a strong control on CV_{ds} . The subalpine study grids were most negatively correlated with the VH and CD variables suggesting that forest structure is important driver of subalpine subgrid variability with increases in forest canopy coverage generally reducing CV_{ds} .

Table 2. Bivariate correlations (Pearson's r coefficient) between snow depth coefficient of variation (CV_{ds}) and the mean and standard deviation (σ) of snow depth (d_s), vegetation height (VH), canopy density (CD), elevation (z), slope (S), winter clear-sky incoming solar radiation ($Q_{sw\downarrow}$), maximum upwind slope (Sx), and topographic position index (TPI) for both alpine and subalpine study grids. Correlations are also shown for the residuals from the detrended nonlinear relation of CV_{ds} and d_s . Bold values represent statistical significance (p value < 0.05)

	CV_{ds} (alpine)	CV_{ds} (subalpine)	CV_{ds} (alpine) d_s residuals	CV_{ds} (subalpine) d_s residuals
d_s	-0.60	-0.45	---	---
σ_{d_s}	-0.06	0.25	---	---
VH	-0.38	-0.48	-0.28	-0.71
σ_{VH}	-0.38	-0.57	-0.24	-0.59
CD	-0.06	-0.32	-0.21	-0.64
σ_{CD}	-0.06	0.30	-0.26	0.50
z	0.17	-0.22	0.32	0.18
σ_z	-0.07	0.09	0.16	0.29
S	-0.03	0.06	0.25	0.28
σ_S	-0.06	0.13	0.37	0.38
$Q_{sw\downarrow}$	0.10	-0.02	-0.07	-0.17
$\sigma_{Q_{sw\downarrow}}$	-0.07	-0.03	0.21	0.21
Sx	0.02	0.08	0.29	0.09
σ_{Sx}	0.07	0.10	0.43	0.28
TPI	0.28	0.11	0.15	0.04
σ_{TPI}	-0.09	0.09	0.29	0.33

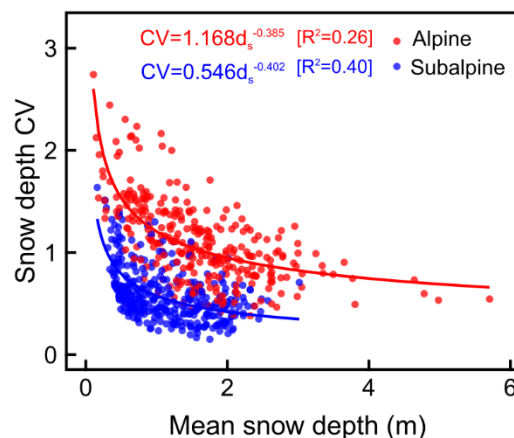


Figure 6. Nonlinear relation of CV_{ds} and d_s for alpine (red) and subalpine (blue) study grids (500 m resolution).

3.4. Statistical models

We evaluated a range of independent variables to be included within the multiple linear regression models (refer to variables in Table 1). However, to make the model analysis most transferable to other mountainous environments, some of the variables were deemed unsuitable and excluded from model testing. For example, mean z was not included in model testing as it was believed to be a site-specific variable that may not have been transferable to independent data. Additionally, VH and σ_{VH} were not tested despite their strong correlation with subalpine CV_{ds} as these variables are not commonly available as spatial datasets, such as the USGS National Land Cover Database

(<http://www.mrlc.gov/index.php>) land cover type and canopy density products. Variables that were shown to significantly improve model diagnostics and performance and suggested relations with CV_{ds} that make physical sense were included in the final models. The multiple linear regression models developed for predicting CV_{ds} in both alpine and subalpine seasonal snowpacks are presented in Table 3. Variable transformations were necessary to CV_{ds} and d_s in both models and to σ_{Sx} in the alpine model and CD in the subalpine model to account for the nonlinearity of these datasets (Table 3). Snow depth exhibited the greatest explanatory ability within both the alpine and subalpine models, with standardized regression coefficients equal to -0.92 and -0.95, respectively (not shown). Standardized regression coefficients of σ_{Sx} and CD were equal to 0.50 and -0.72 for the alpine and subalpine models, respectively, and both showed the second strongest explanatory power in their respective models. For the model calibration dataset (10-fold cross-verification dataset), the alpine model had a NSE of 0.66 (0.65) and RMSE of 0.24 (0.24) while the subalpine model had an NSE of 0.79 (0.78) and RMSE of 0.12 (0.13) (Fig. 7). A total NSE of 0.81 was calculated for the entire dataset based on predictions from both models. These performance statistics suggest that the models perform reasonably well predicting CV_{ds} and cross-verification suggests the model may be transferable to independent data within the bounds of the original dataset.

Table 3. Multiple linear regression equation variables and coefficients of the alpine and subalpine CV_{ds} models. The multiple linear regression is of the form: $y = \beta_0 + \beta_1 X_1 + \beta_2 X_2 + \dots + \beta_n X_n$ where y is the dependent variable, x_1 through x_n are n independent variables, β_0 is the regression intercept, and β_1 through β_n are n regression coefficients.

	Alpine model	Subalpine model
Y	$\log(CV_{ds})$	$CV_{ds}^{0.5}$
β_0	9.00E-03	8.45E-01
β_1	-1.02E+00	-2.84E-01
x_1	$d_s^{0.5}$	$\log(d_s)$
β_2	1.00E-02	-9.79E-05
x_2	Sx	CD^2
β_3	3.42E-01	1.12E-02
x_3	$\log(\sigma_{Sx})$	σ_S
β_4	1.84E-03	---
x_4	$Q_{SW\downarrow}$	---

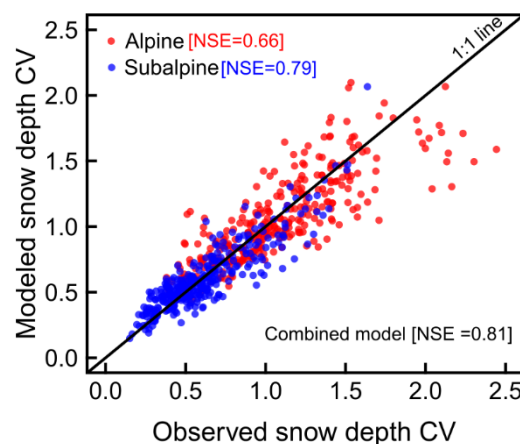


Figure 7. Modeled versus observed CV_{ds} for the alpine (red) and subalpine (blue) multiple linear regression models.

4. Discussion

Based on an evaluation of CV_{ds} at a 500 m grid resolution, subgrid snow variability across a mountainous subalpine and alpine study area is shown to exhibit a wide range of spatial variation and be well correlated with ecosystem type, snow amount, as well as terrain characteristics and forest structure. Alpine CV_{ds} was most correlated with mean snow depth and the variability of exposure to wind while mean snow depth and canopy height and density were most correlated with CV_{ds} in subalpine areas. A statistical model for both alpine and subalpine ecosystems was able to reasonably predict subgrid CV_{ds} based on these relations and could be used to support improving model parameterizations of subgrid snow variability in mountainous terrain.

The range of CV_{ds} observed over relatively small distances in this study (Fig. 5) highlights the importance of further characterizing the spatial variability of this parameter within mountainous terrain. The global classification of CV_{SWE} defined by Liston (2004) performed well predicting the average conditions observed in this study. Liston (2004) define the CV_{SWE} of mid-latitude mountainous forest (i.e. subalpine) as 0.60 and of mid-latitude treeless mountains (i.e. alpine) as 0.85, whereas this study found a median CV_{ds} of 0.55 for subalpine study grids and 1.05 for alpine study grids. However, the global classification was unable to adequately represent the range and variability of CV_{ds} across the study area (Fig. 4c), and the results presented herein further characterize the distribution and variability of CV_{ds} in mountainous terrain.

Mean snow depth was the main driver of CV_{ds} variability across alpine and subalpine areas within the study area. As subgrid d_s increased, the CV_{ds} decreased, which is a result that is consistent with previous studies at various spatial scales (Fassnacht and Deems, 2006; Fassnacht and Hultstrand, 2015; López-Moreno *et al.*, 2015). A positive correlation was observed between σ_{ds} and d_s in alpine and subalpine areas, which had a dampening effect on this overall negative correlation between the relative subgrid variability (CV_{ds}) with d_s . The relative subgrid variability of d_s likely decreases with increasing snow accumulation because of the consistent size of the roughness elements of terrain and canopy that drive snow variability; as d_s increases, the relative influence of these terrain and canopy features tends to decrease (Fassnacht and Deems, 2006; López-Moreno *et al.*, 2011; López-Moreno *et al.*, 2015]. The range of CV_{ds} observed in this study (Fig. 4) is similar to previous studies conducted in mountainous mid-latitude forested and alpine areas [refer to Figure 2 from Clark *et al.*, 2011 and references therein]. Future research could further investigate CV_{ds} and d_s across different geographic regions and snow regimes as well as across multiple snow seasons and compare results to the functions presented in Figure 6 to better understand the dynamics and consistency of this relation. An understanding of how the subgrid variability of snow depth for a given set of terrain and canopy elements scales between low and high snow years could be particularly important.

Within the alpine study grids, the variability of the exposure/sheltering from wind (σ_{sx}) was an important driver of CV_{ds} . Study grids with the greatest σ_{sx} were generally positioned over large breaks in terrain. For example, a given study grid with a large σ_{sx} likely contained areas with both wind exposure ($Sx < 0^\circ$) where snow accumulation is scoured by wind and sheltering from wind ($Sx > 0^\circ$) where preferential deposition of wind transported snow occurs. Study grids with a consistent Sx showed a lower CV_{ds} with greater variability observed in sheltered grids than in exposed grids. Winstral *et al.* (2002) and many subsequent studies (Erickson *et al.*, 2005; Molotch *et al.*, 2005; Revuelto *et al.*, 2014; McGrath *et al.*, 2015) have highlighted this control of wind exposure on snow depth distribution in tree-less areas. The degree of importance of σ_{sx} for describing CV_{ds} is likely variable from year-to-year, and would be expected to be well correlated with observed wind speeds [Winstral and Marks, 2014]. However, in alpine areas where high wind speeds are ubiquitous, σ_{sx} is expected to be a consistently important driver of subgrid snow variability.

Subgrid snow variability within subalpine study grids was well correlated with VH and CD . As mean study grid VH and CD increased, CV_{ds} tended to decrease. Forest structure has been shown by various studies to have a strong influence on snow variability because of a variety of physical process

interactions. Interception of snow (Hedstrom and Pomeroy, 1998; Suzuki and Nakai, 2008] and subsequent canopy sublimation (Montesi *et al.*, 2004; Molotch *et al.*, 2007), influences of trees on shortwave (Ellis and Pomeroy, 2007; Musselman *et al.*, 2012) and longwave (Pomeroy *et al.*, 2009; Yamazaki and Kondo, 1992) radiation dynamics, and the effect of trees on wind redistribution of snow (Hiemstra *et al.*, 2006) can each drive snow accumulation and evolution in forested areas. Broxton *et al.* (2015) utilized lidar-derived snow depth datasets and showed that the variability of snow depth in subalpine forests tended to be greatest beneath the forest canopy and near the forest canopy edge and the least snow depth variability occurred in forested openings that were distant from the forest edge, relating to fetch and area contributing to snow deposition. Also, substantial differences in accumulated d_s were observed between subcanopy areas and forest openings. The increased CV_{d_s} with decreasing VH and CD observed in this study can be explained by a greater occurrence of transitional areas between subcanopy areas and forest openings (i.e., forest edges) occurring in study grids with smaller mean VH and CD . Across the study area, subalpine forest openings that spanned an entire study grid were not present; therefore, study grids with consistent forest cover tended to exhibit the least subgrid snow variability.

This study was limited by the spatial and temporal coverage of the lidar-derived snow datasets that were used (Fig. 1). Although the alpine and subalpine areas evaluated are representative of mountainous terrain in the region and snowpacks in this area are representative of the continental snow regime (Trujillo and Molotch, 2014), further analysis of subgrid snow variability across a greater geographic area and across other regions with differing snow regimes could improve the applicability of a CV_{d_s} parameterization for snow distributions in mountains areas in general. Additionally, spatial patterns of snow variability have been shown to be temporally consistent from year-to-year (Erickson *et al.*, 2005; Deems *et al.*, 2008; Sturm and Wagner, 2010], but future studies with multiple years of lidar collection could help understand the inter-annual variability of CV_{d_s} and the consistency of its driving variables (Fassnacht *et al.*, 2012]. Of particular interest would be the temporal consistency of the relation between CV_{d_s} and d_s .

This study evaluates the subgrid variability of d_s , but SWE is the most fundamental snowpack variable of interest in land surface processes (Sturm *et al.*, 2010). Snow depth and SWE have been shown by many studies to be well correlated (Jonas *et al.*, 2009; Sturm *et al.*, 2010; Sexstone and Fassnacht, 2014), and the subgrid CV of these variables is expected to exhibit similar characteristics (Fassnacht and Hultstrand, 2015). We suggest that a parameterization of CV_{d_s} could be sufficient for representing subgrid SWE variability, but further investigation into this hypothesis is needed. In order to directly investigate CV_{SWE} from lidar-derived snow data in future studies, an estimation of snow density would be needed. Statistically-derived snow density models have been successfully developed over varying domain sizes for estimating SWE from d_s (Jonas *et al.*, 2009; Sturm *et al.*, 2010; Sexstone and Fassnacht, 2014), and these models make use of the fact that SWE and d_s variability is much greater than the variability of snow density (Mizukami and Perica, 2008; Lopez-Moreno *et al.*, 2013).

The snow distributions and variability characteristics evaluated in this study were likely influenced by the occurrence of snowmelt conditions within the study area. Although substantial snowmelt had not occurred prior to data collection within the study grids (Figure 2), the mid-season melt events and onset of snowmelt may have caused an increase in CV_{d_s} and this effect may have differed between the two dates of lidar-derived d_s . López-Moreno *et al.* (2015) observed a sharp increase in CV_{d_s} just following the onset of snowmelt yet a fairly consistent CV_{d_s} for the remainder of snowmelt season. Future studies evaluating subgrid snow variability should investigate the intra-annual variability CV_{d_s} to further understand the seasonal evolution of this parameter.

The development of high-resolution snow depth mapping from lidar has provided a unique ability for detailed snapshot views of the spatial distribution of snow in complex mountains areas. Although some key advantages of these datasets are related to validating satellite-based remote sensing products and direct use within water resources forecasting, this study also suggests that lidar-derived

snow datasets can be an important tool for the improvement of snow representations within modeling applications. Future research should utilize lidar-derived snow datasets to directly evaluate the ability of physically-based models to represent snow distributions as well as to continue to improve the representation of subgrid variability of snow. Additionally, other key snow modeling questions such as how representative snow monitoring stations are of surrounding areas (Molotch and Bales, 2005; Meromy *et al.*, 2013) could also be investigated further by lidar-derived snow datasets. Lastly, the analysis methods that have been developed in this study may also be useful in future studies for characterizing the subgrid variability of other variables that can be measured remotely at a fine scale through lidar or other measurement techniques.

5. Conclusions

This study outlines a methodology for utilizing lidar-derived snow datasets for investigating subgrid snow depth (d_s) variability and potentially improving its representation within physically-based modeling applications. At fine grid resolutions, subgrid snow depth coefficient of variation (CV_{d_s}) generally increased and its variability decreased with increasing grid resolution, while study grid CV_{d_s} characteristics were similar among a range of coarser resolutions (from 500 m to 1000 m). Study grids (500 m resolution) exhibited a wide range of CV_{d_s} across the study area (0.15 to 2.74) and subgrid d_s variability was found to be greater in alpine areas than subalpine areas. Snow depth was the most important driver of CV_{d_s} variability in both alpine and subalpine areas and a systematic nonlinear decrease in CV_{d_s} with increasing d_s was observed; the negative correlation between CV_{d_s} and d_s is attributed to the static size of roughness elements (terrain and canopy) that strongly influence seasonal snow variability. The variability of wind exposure in alpine areas as well as mean vegetation height and canopy density in subalpine areas were also found to be important drivers of study grid CV_{d_s} . Two statistical models were developed (alpine and subalpine) for predicting subgrid CV_{d_s} from mean d_s and terrain/canopy features. They show reasonably good performance statistics and suggest this methodology can be used for characterizing CV_{d_s} in snow-dominated mountainous areas. This research highlights the utility of using lidar-derived snow datasets for improving model representations of subgrid snow variability.

Acknowledgements

This work was partially funded by the NASA Terrestrial Hydrology Program (award NNX11AQ66G ‘Improved Characterization of Snow Depth in Complex Terrain Using Satellite Lidar Altimetry’ PI Michael F. Jasinski NASA GSFC). The airborne lidar data were collected in collaboration between the Boulder Creek CZO and the National Center for Airborne Laser Mapping, both of which are funded by the National Science Foundation. The lidar-derived elevation, vegetation, and snow datasets were processed and made publicly available as described in Harpold *et al.* [2014] and were invaluable datasets for this study. Thanks to Adam Winstal for providing the *Sx* code.

References

- Akaike, H. 1974. A new look at the statistical model identification. *IEEE Transactions on Automatic Control* 19(6), 716-723. <https://doi.org/10.1109/TAC.1974.1100705>
- Berris, S.N., Harr, R.D. 1987. Comparative snow accumulation and melt during rainfall in forested and clear-cut plots in the Western Cascades of Oregon. *Water Resources Research* 23(1), 135–142. <https://doi.org/10.1029/WR023i001p00135>
- Bierkens, M.F.P., Bell, V.A., Burek, P., Chaney, N., Condon, L.E., David, C.H., de Roo, A., Döll, P.P.D., Drost, N., Famiglietti, J.S., Flörke, M., Gochis, D.J., Houser, P., Hut, R., Keune, J., Kollet, S., Maxwell, R.M., Reager, J.T., Samaniego, L., Sudicky, E., Sutanudjaja, E.H., van de Giesen, N., Winsemius, H., Wood,

- E.F. 2015. Hyper-resolution global hydrological modelling: what is next? "Everywhere and locally relevant". *Hydrological Processes* 29 (2), 310-320. <https://doi.org/10.1002/hyp.10391>
- Blöschl, G. 1999. Scaling issues in snow hydrology. *Hydrological Processes* 13 (14-15), 2149-2175. [https://doi.org/10.1002/\(SICI\)1099-1085\(199910\)13:14/15<2149::AID-HYP847>3.0.CO;2-8](https://doi.org/10.1002/(SICI)1099-1085(199910)13:14/15<2149::AID-HYP847>3.0.CO;2-8)
- Broxton, P.D., Harpold, A.A., Biederman, J.A., Troch, P.A., Molotch, N.P., Brooks, P.D. 2015. Quantifying the effects of vegetation structure on snow accumulation and ablation in mixed-conifer forests. *Ecohydrology* 8 (6), 1073-1094. <https://doi.org/10.1002/eco.1565>
- Bühler, Y., Marty, M., Egli, L., Veitinger, J., Jonas, T., Thee, P., Ginzler, C. 2015. Snow depth mapping in high-alpine catchments using digital photogrammetry. *The Cryosphere* 9 (1), 229-243. <https://doi.org/10.5194/tc-9-229-2015>
- Carroll, T., Cline, D., Olheiser, C., Rost, A., Nilsson, A., Fall, G., Bovitz, C., Li, L. 2006. NOAA's National Snow Analyses, paper presented at *74th Annual Western Snow Conference*, Las Cruces, NM.
- Clark, M.P., Hendrikx, J., Slater, A.G., Kavetski, D., Anderson, B., Cullen, N.J., Kerr, T., Hreinsson, E.O., Woods, R.A. 2011. Representing spatial variability of snow water equivalent in hydrologic and land-surface models: A review. *Water Resources Research* 47 (7). <https://doi.org/10.1029/2011WR010745>
- Deems, J.S., Fassnacht, S.R., Elder, K.J. 2006. Fractal distribution of snow depth from Lidar data. *Journal of Hydrometeorology* 7 (2), 285-297. <https://doi.org/10.1175/JHM487.1>
- Deems, J.S., Fassnacht, S.R., Elder, K.J. 2008. Interannual consistency in fractal snow depth patterns at Two Colorado Mountain Sites. *Journal of Hydrometeorology* 9 (5), 977-988. <https://doi.org/10.1175/2008JHM901.1>
- Deems, J.S., Painter, T.H., Finnegan, D.C. 2013. Lidar measurement of snow depth: a review. *Journal of Glaciology* 59 (215), 467-479. <https://doi.org/10.3189/2013Jog12J154>
- Egli, L., Jonas, T. 2009. Hysteretic dynamics of seasonal snow depth distribution in the Swiss Alps. *Geophysical Research Letters*, 36 (2), L02501. <https://doi.org/10.1029/2008GL035545>
- Elder, K., Rosenthal, W., Davis, R.E. 1998. Estimating the spatial distribution of snow water equivalence in a montane watershed. *Hydrological Processes* 12 (10-11), 1793-1808. [https://doi.org/10.1002/\(SICI\)1099-1085\(199808/09\)12:10/11<1793::AID-HYP695>3.0.CO;2-K](https://doi.org/10.1002/(SICI)1099-1085(199808/09)12:10/11<1793::AID-HYP695>3.0.CO;2-K)
- Ellis, C.R., Pomeroy, J.W. 2007. Estimating sub-canopy shortwave irradiance to melting snow on forested slopes. *Hydrological Processes* 21(19), 2581-2593. <https://doi.org/10.1002/hyp.6794>
- Erickson, T.A., Williams, M.W., Winstral, A. 2005. Persistence of topographic controls on the spatial distribution of snow in rugged mountain terrain, Colorado, United States, *Water Resources Research* 41 (4). <https://doi.org/10.1029/2003wr002973>
- Fassnacht, S.R., Deems, J.S. 2006. Measurement sampling and scaling for deep montane snow depth data. *Hydrological Processes* 20 (4), 829-838. <https://doi.org/10.1002/hyp.6119>
- Fassnacht, S.R., Dressler, K.A., Hultstrand, D.M., Bales, R.C., Patterson, G. 2012. Temporal inconsistencies in coarse-scale snow water equivalent patterns: Colorado River Basin snow telemetry-topography regressions. *Pirineos* 167(0), 165-185. <https://doi.org/10.3989/Pirineos.2012.167008>
- Fassnacht, S.R., Hultstrand, M. 2015. Snowpack variability and trends at long-term stations in northern Colorado, USA. *Proceedings of the International Association of Hydrological Sciences* 371, 131-136. <https://doi.org/10.5194/piahs-371-131-2015>
- Grünewald, T., Schirmer, M., Mott, R., Lehning, M. 2010. Spatial and temporal variability of snow depth and ablation rates in a small mountain catchment. *The Cryosphere* 4 (2), 215-225. <https://doi.org/10.5194/tc-4-215-2010>
- Grünewald, T., Stötter, J., Pomeroy, J.W., Dadić, R., Moreno Baños, I., Marturià, J., Spross, M., Hopkinson, C., Burlando, P., Lehning, M. 2013. Statistical modelling of the snow depth distribution in open alpine terrain. *Hydrology and Earth System Sciences* 17 (8), 3005-3021. <https://doi.org/10.5194/hess-17-3005-2013>

- Harpold, A.A., Guo, Q., Molotch, N., Brooks, P.D., Bales, R., Fernandez-Diaz, J.C., Musselman, K.N., Swetnam, T.L., Kirchner, P., Meadows, M.W., Flanagan, J., Lucas, R. 2014. LiDAR-derived snowpack data sets from mixed conifer forests across the Western United States. *Water Resources Research* 50 (3), 2749-2755. <https://doi.org/10.1002/2013WR013935>
- Hedstrom, N.R., Pomeroy, J.W. 1998. Measurements and modelling of snow interception in the boreal forest. *Hydrological Processes* 12(10-11), 1611-1625. [https://doi.org/10.1002/\(SICI\)1099-1085\(199808/09\)12:10<11%3C1611::AID-HYP684%3E3.0.CO;2-4](https://doi.org/10.1002/(SICI)1099-1085(199808/09)12:10<11%3C1611::AID-HYP684%3E3.0.CO;2-4)
- Hiemstra, C.A., Liston, G.E., Reiners, W.A. 2006. Observing, modelling, and validating snow redistribution by wind in a Wyoming upper treeline landscape. *Ecological Modelling* 197 (1-2), 35-51. <https://doi.org/10.1016/j.ecolmodel.2006.03.005>
- Jonas, T., Marty, C., Magnusson, J. 2009. Estimating the snow water equivalent from snow depth measurements in the Swiss Alps. *Journal of Hydrology* 378 (1-2), 161-167. <https://doi.org/10.1016/j.jhydrol.2009.09.021>
- Kerr, T., Clark, M., Hendrikx, J., Anderson, B. 2013. Snow distribution in a steep mid-latitude alpine catchment. *Advances in Water Resources* 55, 17-24. <https://doi.org/10.1016/j.advwatres.2012.12.010>
- Kirchner, P. B., Bales, R. C., Molotch, N. P., Flanagan, J., Guo, Q. 2014. LiDAR measurement of seasonal snow accumulation along an elevation gradient in the southern Sierra Nevada, California. *Hydrology and Earth System Sciences*, 18 (10), 4261-4275. <https://doi.org/10.5194/hess-18-4261-2014>
- Kumar, S.V., Peters-Lidard, C.D., Tian, Y., Houser, P.R., Geiger, J., Olden, S., Lighty, L., Eastman, J.L., Doty, B., Dirmeyer, P., Adams, J., Mitchell, K., Wood, E.F., Sheffield, J. 2006. Land information system: An interoperable framework for high resolution land surface modeling. *Environmental Modelling & Software* 21 (10), 1402-1415. <https://doi.org/10.1016/j.envsoft.2005.07.004>
- Liston, G.E. 1999. Interrelationships among snow distribution, snowmelt, and snow cover depletion: Implications for atmospheric, hydrologic, and ecologic modeling. *Journal of Applied Meteorology* 38 (10), 1474-1487. [https://doi.org/10.1175/1520-0450\(1999\)038<1474:IASDSA>2.0.CO;2](https://doi.org/10.1175/1520-0450(1999)038<1474:IASDSA>2.0.CO;2)
- Liston, G.E. 2004. Representing subgrid snow cover heterogeneities in regional and global models. *Journal of Climate* 17 (6), 1381-1397. [https://doi.org/10.1175/1520-0442\(2004\)017<1381:RSSCHI>2.0.CO;2](https://doi.org/10.1175/1520-0442(2004)017<1381:RSSCHI>2.0.CO;2)
- Liston, G.E., Hiemstra, C.A. 2011. Representing Grass- and Shrub-Snow-Atmosphere Interactions in Climate System Models. *Journal of Climate* 24 (8), 2061-2079. <https://doi.org/10.1175/2010JCLI4028.1>
- López-Moreno, J.I., Fassnacht, S.R., Beguería, S., Latron, J.B.P. 2011. Variability of snow depth at the plot scale: implications for mean depth estimation and sampling strategies. *The Cryosphere* 5 (3), 617-629. <https://doi.org/10.5194/tc-5-617-2011>
- Lopez-Moreno, J.I., Fassnacht, S.R., Heath, J.T., Musselman, K.N., Revuelto, J., Latron, J., Moran-Tejeda, E., Jonas, T. 2013. Small scale spatial variability of snow density and depth over complex alpine terrain: Implications for estimating snow water equivalent. *Advances in Water Resources* 55, 40-52. <https://doi.org/10.1016/j.advwatres.2012.08.010>
- López-Moreno, J.I., Revuelto, J., Fassnacht, S.R., Azorín-Molina, C., Vicente-Serrano, S.M., Morán-Tejeda, E., Sexstone, G.A. 2015. Snowpack variability across various spatio-temporal resolutions. *Hydrological Processes*, 29 (6), 1213-1224. <https://doi.org/10.1002/hyp.10245>
- Mallows, C.L. 1973. Some Comments on Cp. *Technometrics* 15 (4), 661.
- McGrath, D., Sass, L., O'Neel, S., Arendt, A., Wolken, G., Gusmeroli, A., Kienholz, C., McNeil C. 2015. End-of-winter snow depth variability on glaciers in Alaska. *Journal of Geophysical Research: Earth Surface* 120 (8), 1530-1550. <https://doi.org/10.1002/2015JF003539>
- Meromy, L., Molotch, N.P., Link, T.E., Fassnacht, S.R., Rice, R. 2013. Subgrid variability of snow water equivalent at operational snow stations in the western USA. *Hydrological Processes* 27 (17), 2383-2400. <https://doi.org/10.1002/hyp.9355>
- Mizukami, N., Perica, S. 2008. Spatiotemporal characteristics of snowpack density in the mountainous regions of the Western United States. *Journal of Hydrometeorology* 9 (6), 1416-1426. <https://doi.org/10.1175/2008JHM981.1>

- Molotch, N.P., Bales, R.C. 2005. Scaling snow observations from the point to the grid element: Implications for observation network design. *Water Resources Research* 41 (11), W11421. <https://doi.org/10.1029/2005WR004229>
- Molotch, N.P., Colee, M.T., Bales, R.C., Dozier, J. 2005. Estimating the spatial distribution of snow water equivalent in an alpine basin using binary regression tree models: the impact of digital elevation data and independent variable selection. *Hydrological Processes* 19 (7), 1459-1479. <https://doi.org/10.1002/hyp.5586>
- Molotch, N.P., Blanken, P.D., Williams, M.W., Turnipseed, A.A., Monson, R.K., Margulis, S.A. 2007. Estimating sublimation of intercepted and sub-canopy snow using eddy covariance systems. *Hydrological Processes* 21 (12), 1567-1575. <https://doi.org/10.1002/hyp.6719>
- Montesi, J., Elder, K., Schmidt, R.A., Davis, R.E. 2004. Sublimation of intercepted snow within a Subalpine Forest Canopy at Two Elevations. *Journal of Hydrometeorology* 5 (5), 763-773. [https://doi.org/10.1175/1525-7541\(2004\)005<0763:SOISWA>2.0.CO;2](https://doi.org/10.1175/1525-7541(2004)005<0763:SOISWA>2.0.CO;2)
- Musselman, K.N., Molotch, N.P., Margulis, S.A., Kirchner, P.B., Bales, R.C. 2012. Influence of canopy structure and direct beam solar irradiance on snowmelt rates in a mixed conifer forest. *Agricultural and Forest Meteorology* 161, 46-56. <https://doi.org/10.1016/j.agrformet.2012.03.011>
- Nolan, M., Larsen, C., Stur, M. 2015. Mapping snow depth from manned aircraft on landscape scales at centimeter resolution using structure-from-motion photogrammetry. *The Cryosphere*, 9 (4), 1445-1463. <https://doi.org/10.5194/tc-9-1445-2015>
- Pomeroy, J.W., Gray, D.M., Shook, K.R., Toth, B., Essery, R.L.H., Pietroniro, A., Hedstrom, N. 1998. An evaluation of snow accumulation and ablation processes for land surface modelling. *Hydrological Processes* 12 (15), 2339-2367. [https://doi.org/10.1002/\(SICI\)1099-1085\(199812\)12:15<2339::AID-HYP800>3.0.CO;2-L](https://doi.org/10.1002/(SICI)1099-1085(199812)12:15<2339::AID-HYP800>3.0.CO;2-L)
- Pomeroy, J.W., Marks, D., Link, T., Ellis, C., Hardy, J., Rowlands, A., Granger, R. 2009. The impact of coniferous forest temperature on incoming longwave radiation to melting snow. *Hydrological Processes* 23 (17), 2513-2525. <https://doi.org/10.1002/hyp.7325>
- Revuelto, J., López-Moreno, J.I., Azorin-Molina, C., Vicente-Serrano, S.M. 2014. Topographic control of snowpack distribution in a small catchment in the central Spanish Pyrenees: intra- and inter-annual persistence. *The Cryosphere* 8 (5), 1989-2006. <https://doi.org/10.5194/tc-8-1989-2014>
- Revuelto, J., Lopez-Moreno, J.I., Azorin-Molina, C., Vicente-Serrano, S. M. 2015. Canopy influence on snow depth distribution in a pine stand determined from terrestrial laser data. *Water Resources Research* 51 (5), 3476-3489. <https://doi.org/10.1002/2014WR016496>
- Richer, E.E., Kampf, S.K., Fassnacht, S.R., Moore, C.C. 2013. Spatiotemporal index for analyzing controls on snow climatology: application in the Colorado Front Range. *Physical Geography* 34 (2), 85-107. <https://doi.org/10.1080/02723646.2013.787578>
- Sexstone, G.A., Fassnacht, S.R. 2014. What drives basin scale spatial variability of snowpack properties in northern Colorado? *The Cryosphere* 8 (2), 329-344. <https://doi.org/10.5194/tc-8-329-2014>
- Seyfried, M.S., Wilcox, B.P. 1995. Scale and the nature of spatial variability - Field examples having implications for hydrologic modeling. *Water Resources Research* 31 (1), 173-184. <https://doi.org/10.1029/94WR02025>
- Slater, A.G., Schlosser, C.A., Desborough, C.E., Pitman, A.J., Henderson-Sellers, A., Robock, A., Ya Vinnikov, K., Entin, J., Mitchell, K., Chen, F., Boone, A., Etchevers, P., Habets, F., Noilhan, J., Braden, H., Cox, P.M., de Rosnay, P., Dickinson, R.E., Yang, Z-L, Dai, Y-J, Zeng, Q., Duan, Q., Koren, V., Schaake, S., Gedney, N., Gusev, Ye M., Nasonova, O.N., Kim, J., Kowalczyk, E.A., Shmakin, A.-B., Smirnova, T.G., Verseghy, D., Wetzel, P., Xue, Y. 2001, The representation of snow in land surface schemes: Results from PILPS 2(d). *Journal of Hydrometeorology* 2 (1), 7-25. [https://doi.org/10.1175/1525-7541\(2001\)002<0007:TROSIL>2.0.CO;2](https://doi.org/10.1175/1525-7541(2001)002<0007:TROSIL>2.0.CO;2)
- Sturm, M., Holmgren, J., Liston, G.E. 1995. A seasonal snow cover classification-system for local to global applications. *Journal of Climate* 8 (5), 1261-1283. [https://doi.org/10.1175/1520-0442\(1995\)008<1261:ASSCCS>2.0.CO;2](https://doi.org/10.1175/1520-0442(1995)008<1261:ASSCCS>2.0.CO;2)

- Sturm, M., Wagner, A.M. 2010. Using repeated patterns in snow distribution modeling: An Arctic example. *Water Resources Research* 46 (12), W12549. <https://doi.org/10.1029/2010WR009434>
- Sturm, M., Taras, B., Liston, G.E., Derksen, C., Jonas, T., Lea, J. 2010. Estimating snow water equivalent using snow depth data and climate classes. *Journal of Hydrometeorology* 11 (6), 1380-1394. <https://doi.org/10.1175/2010JHM1202.1>
- Suding, K.N., Farrer, E.C., King, A.J., Kueppers, L., Spasojevic, M.J. 2015. Vegetation change at high elevation: scale dependence and interactive effects on Niwot Ridge. *Plant Ecology & Diversity* 8 (5-6), 713-725. <https://doi.org/10.1080/17550874.2015.1010189>
- Suzuki, K., Nakai, Y. 2008. Canopy snow influence on water and energy balances in a coniferous forest plantation in northern Japan. *Journal of Hydrology* 352, 126-138. <https://doi.org/10.1016/j.jhydrol.2008.01.007>
- Trujillo, E., Ramirez, J.A., Elder, K.J. 2007. Topographic, meteorologic, and canopy controls on the scaling characteristics of the spatial distribution of snow depth fields. *Water Resources Research*, 43 (7), W07409. <https://doi.org/10.1029/2006WR005317>
- Trujillo, E., Molotch, N P. 2014. Snowpack regimes of the Western United States. *Water Resources Research* 50 (7), 5611-5623. <https://doi.org/10.1002/2013WR014753>
- Trujillo, E., Lehning, M. 2015. Theoretical analysis of errors when estimating snow distribution through point measurements. *The Cryosphere* 9, 1249-1264. <https://doi.org/10.5194/tc-9-1249-2015>
- Weiss, A.D. 2001. Topographic position and landforms analysis, in *ESRI User Conference*, edited, San Diego, USA.
- Winstral, A., Elder, K., Davis, R.E. 2002. Spatial snow modeling of wind-redistributed snow using terrain-based parameters. *Journal of Hydrometeorology* 3 (5), 524-538. [https://doi.org/10.1175/1525-7541\(2002\)003<0524:SSMOWR>2.0.CO;2](https://doi.org/10.1175/1525-7541(2002)003<0524:SSMOWR>2.0.CO;2)
- Winstral, A., Marks, D. 2014. Long-term snow distribution observations in a mountain catchment: Assessing variability, time stability, and the representativeness of an index site. *Water Resources Research* 50 (1), 293-305. <https://doi.org/10.1002/2012WR013038>
- Wood, E.F., Roundy, J.K., Troy, T.J., van Beek, L. P.H., Bierkens, M.F.P., Blyth, E., de Roo, A., Döll, P., Ek, M., Famiglietti, J., Gochis, D., van de Giesen, N., Houser, P., Jaffé, P.R., Kollet, S., Lehner, B., Lettenmaier, D.P., Peters-Lidard, C., Sivapalan, M., Sheffield, J., Wade, A., Whitehead, P. 2011. Hyperresolution global land surface modeling: Meeting a grand challenge for monitoring Earth's terrestrial water. *Water Resources Research* 47 (5). <https://doi.org/10.1029/2010WR010090>
- Yamazaki, T., Kondo, J., Watanabe, T., Sato, T. 1992. A heat-balance model with a canopy of one or two layers and its application to field experiments. *Journal of Applied Meteorology and Climatology* 31, 86-103. [https://doi.org/10.1175/1520-0450\(1992\)031<0086:AHBMWA>2.0.CO;2](https://doi.org/10.1175/1520-0450(1992)031<0086:AHBMWA>2.0.CO;2)
- Yang, Z.L., Dickinson, R.D., Robock, A., Vinnikov, K.Y. 1997. Validation of the snow submodel of the biosphere-atmosphere transfer scheme with Russian snow cover and meteorological observational data. *Journal of Climate* 10 (2), 353-373. [https://doi.org/10.1175/1520-0442\(1997\)010<0353:VOTSSO>2.0.CO;2](https://doi.org/10.1175/1520-0442(1997)010<0353:VOTSSO>2.0.CO;2)
- Zheng, Z., Kirchner, P.B., Bales, R.C. 2016. Topographic and vegetation effects on snow accumulation in the southern Sierra Nevada: a statistical summary from lidar data. *The Cryosphere* 10 (1), 257-269. <https://doi.org/10.5194/tc-10-257-2016>